

A Hybrid Cellular Automaton Model of Smoldering
Propagation in Forest Floor Duff

Benjamin V. Holt^{1†}, bvh6@humboldt.edu

Elizabeth A. Burroughs^{1,2}, burrough@math.montana.edu

J. Morgan Varner III³, jmvarner@humboldt.edu

Christopher J. Dugaw¹, dugaw@humboldt.edu

¹ Department of Mathematics, Humboldt State University,
1 Harpst Street, Arcata, CA, 95521, USA

² Department of Mathematical Sciences, Montana State University,
Bozeman, MT, 59717-2400, USA

³ Department of Forestry and Wildland Resources, Humboldt State University,
1 Harpst Street, Arcata, CA, 95521, USA

†Corresponding author.

Department of Mathematics, Humboldt State University,
1 Harpst Street, Arcata, CA, 95521, USA
phone 707-826-4020. fax 707-826-3140

1

Abstract

2

3

4

5

6

7

8

9

10

11

12

13

14

15

16

17

18

19

20

This study presents a general spatial model for the consumption of forest floor duff by smoldering combustion. Smoldering ground fires have an enormous impact upon the ecology and management of forest lands throughout the temperate zone. Here we propose a model to predict and better understand observed spatial patterns in duff consumption. The model avoids shortcomings often suffered by other models of duff consumption, such as site specificity, by using a small number of user-determined parameters (organic bulk density, moisture content, inorganic content, and duff depth) that can be estimated exclusively from field samples. A two-dimensional hybrid cellular automaton, coupling stochastic and deterministic processes, models the fuel bed. The model returns the stage of combustion, temperature, and moisture content across space and through time. Model output compares favorably to empirical and field studies concerning spatial aspects of duff consumption, predicting expected qualitative features. Modifications to the model are proposed that would advance understanding of the ecological impact of duff consumption.

Keywords: Duff consumption, smoldering combustion, organic soil, spatial heterogeneity, hybrid cellular automata, stochastic model.

21 **Introduction**

22 In recent years, the consumption of forest floor duff by smoldering combus-
23 tion has come to be recognized as a vital component of the ecology and
24 management of forest lands (Miyaniishi 2001). In fire-excluded ecosystems,
25 thick accumulations of duff have profoundly altered forest ecology in addition
26 to contributing to high fuel loads (Miyaniishi 2001; Varner et al. 2005; Hiers
27 et al. 2007). Reducing these accumulations by prescribed burning, however,
28 often presents serious difficulties since accumulated duff may smolder at the
29 base of tree stems for hours leading to unacceptably high tree mortality
30 (Ryan and Frandsen 1991; Swezy and Agee 1991; Varner et al. 2005, 2007).
31 Additionally, smoldering duff may also cause secondary flaming combustion
32 in other types of fuels leading to secondary fire fronts (Frandsen 1991).

33 Ignition of duff may occur either by direct contact with flaming litter
34 or with organic debris that exhibit extended flaming combustion, partic-
35 ularly fallen branches and pine cones (Frandsen 1991; Fonda and Varner
36 2004). When ignition occurs, duff smolders down to the mineral soil leaving
37 it exposed, resulting in a slow, outwardly propagating smoldering perimeter,
38 exposing more mineral soil as it moves (Frandsen 1991). Extinction occurs
39 when the smoldering front reaches conditions not suited to smoldering com-
40 bustion: high moisture content and/or high inorganic content. If the heat
41 generated by smoldering does not exceed the latent heat of vaporization
42 required to drive the moisture from the duff, smoldering cannot continue
43 (Frandsen 1991). Also, inorganic material does not burn and only absorbs
44 heat energy so mineral content is also a limiting factor in the smoldering

45 process of forest duff (Frandsen 1991). The above processes reveal why
46 moisture and mineral content are good predictors of the behavior of smol-
47 dering combustion in duff; two other predictors include the bulk density of
48 organic material in the duff and duff thickness (Frandsen 1997; Miyanishi
49 and Johnson 2002). These four duff characteristics are good predictors of the
50 likelihood of consumption (Frandsen 1987, 1997; Miyanishi 2001; Miyanishi
51 and Johnson 2002).

52 Smoldering combustion in materials such as polymer foams, sawdust,
53 and tobacco has been studied both empirically and by explicitly model-
54 ing the combustion process (Bradbury et al. 1979; Ohlemiller 2002), but
55 few, if any, address forest duff. Studies that specifically seek to understand
56 duff consumption (Frandsen 1987, 1991, 1997, 1998; Miyanishi and Johnson
57 2002) often use peat as the material of study since peat has a high organic
58 content and is structurally similar to forest duff (Frandsen 1987, 1991, 1998;
59 Miyanishi 2001). Frandsen (1987, 1991, 1998) repeatedly notes that peat has
60 similar structural characteristics to forest duff including particle size distri-
61 butions. Miyanishi (2001) also cites studies showing that peat is chemically
62 similar to the fermentation horizon in duff.

63 Here we develop a spatially explicit model for smoldering propagation
64 through a fuel bed. Due to the complexity of combustion chemistry and the
65 consequent difficulties in modeling combustion deterministically, propaga-
66 tion of the smoldering front is taken to be a stochastic process based upon
67 conditions of the unconsumed duff. The ignition probability statement of
68 Frandsen (1997) is used to determine the likelihood of propagation.

69 Since conditions ahead of the front change in time, particularly duff

70 moisture, it is necessary to model how the smoldering front imparts thermal
71 energy to unconsumed duff. The model of Campbell et al. (1995), which
72 is based upon the classic heat and moisture transport model of de Vries
73 (1958), is a one-dimensional model of these processes in soils with high
74 temperatures. The model developed here modifies the Campbell model to
75 account for coupled heat and moisture transport in two dimensions.

76 Our objective was to construct a general model of forest floor duff con-
77 sumption that is easy to use, modify, and incorporate into existing fire be-
78 havior models. To these ends, the model requires only eight parameters
79 determined by the duff.

80 **Methods**

81 The fuel bed is modeled by a two-dimensional hybrid cellular automaton
82 coupling stochastic and deterministic processes (Figure 1). A cellular au-
83 tomaton is a multi-dimensional lattice of cells that are updated in discrete
84 time. The “hybrid” nomenclature emphasizes the interaction between de-
85 terministic and stochastic processes on the lattice. Hybrid cellular automata
86 have been successfully applied to other important phenomena including tu-
87 mor growth (Gerlee and Anderson 2007). To distinguish it from other models
88 of smoldering propagation through a fuel bed, the model developed here will
89 be referred to as the HCA model. In the HCA model, associated with each
90 cell is a *state*. The state of each cell (representing a small patch of duff) is
91 updated using information about itself and its *four nearest neighbors* (Figure
92 2).

93 The state of each cell is represented by a vector whose components are
 94 duff conditions that change in time: the stage of combustion; gravimet-
 95 ric moisture content (GMC); volumetric moisture content (VMC); and duff
 96 temperature. The combustion stage is updated stochastically (Figure 3)
 97 while the latter three are updated deterministically. Also associated with
 98 each cell are quantities that do not change in time: organic bulk density,
 99 mineral content, and duff thickness. Here, the lattice of cells is a square grid
 100 of uniformly spaced points in a plane with cell (1,1) acting as the origin.
 101 The vertical and horizontal distance between adjacent cells is denoted by
 102 Δx so that cell (i, j) occupies the point $(x_i, y_j) = ((i - 1)\Delta x, (j - 1)\Delta x)$.
 103 Each lattice point is interpreted as a small $\Delta x \times \Delta x$ area of duff (Figure 2).
 104 For a broad introduction to stochastic spatial models see Durrett (1999).

105 The combustion process in each cell is modeled by three stages: un-
 106 burned, burning, and burned (Figure 3). Only cells undergoing combustion
 107 can ignite unconsumed cells. If one or more nearest neighbors of an uncon-
 108 sumed cell are burning, then the cell will undergo a transition from unburned
 109 to burning with a probability determined by the conditions of the cell. This
 110 probability is a maximum probability χ that is scaled back by the igni-
 111 tion probability statement given by Frandsen (1997) and depends upon duff
 112 conditions (Equation (1)). Thus the ignition probability of a cell having
 113 gravimetric moisture content γ , mineral content α , and organic bulk density
 114 ρ is assumed to be

$$(1) \quad \mathcal{P}(\text{Ignition}) = \frac{\chi}{1 + e^{-(B_0 + B_1\gamma + B_2\alpha + B_3\rho)}}.$$

115 The parameters B_0 , B_1 , B_2 , B_3 are estimated using logistic regression on
 116 burn/no-burn data for a particular type of duff. The probability χ deter-
 117 mines an uninhibited smolder velocity on the lattice. To calibrate the model
 118 to achieve a desired uninhibited smolder velocity (oven dry duff), the model
 119 is allowed to run multiple times with particular values for the ignition prob-
 120 ability χ , spacing Δx , and update interval Δt . The smolder velocity is then
 121 taken to be the mean of a sufficient number of trials. With data for smolder
 122 velocity for varying values of the parameters χ , Δx , and Δt , the smolder
 123 velocity, Λ , is statistically modeled in terms of these parameters. Solving for
 124 χ in the resulting model yields an expression for the probability that gives
 125 the desired uninhibited smolder velocity:

$$\chi = \frac{\Delta t}{S_1 \Delta x} (\Lambda - S_0 - S_2 \Delta x - S_3 \Delta t),$$

126 where $S_0 = 0.0021$, $S_1 = 1.90$, $S_2 = -0.00476$, and $S_3 = -0.00185$.

127 Once a cell transitions from unburned to burning, the HCA model de-
 128 termines how long it burns. If a cell is burning, it will continue to burn
 129 provided there is fuel to be consumed and will pass to the burned state
 130 when no fuel remains. Instead of modeling directly the consumption of fuel,
 131 the time a cell undergoes combustion is assumed to be exponentially dis-
 132 tributed with mean λ (Ross 2005). The mean smoldering time λ is assumed
 133 to be proportional to the amount of time it takes for a smoldering front to
 134 travel the distance Δx on the lattice which is on average $\frac{\Delta x}{\Lambda}$. This average
 135 smoldering time is then scaled by a dimensionless proportionality constant
 136 ϑ so that $\lambda = \vartheta \frac{\Delta x}{\Lambda}$.

137 Duff moisture is necessary for determining the ignition probability in
138 unconsumed cells. Consequently, the HCA model monitors the amount of
139 thermal energy imparted to the unconsumed duff by the smoldering front
140 that then drives off moisture in neighboring cells. Therefore, the tempera-
141 ture T (Kelvin) of the duff for each time step is calculated. Duff thickness
142 influences the efficiency at which the smoldering front imparts thermal en-
143 ergy to unconsumed duff. Thus also associated with each cell is a thickness
144 τ (m). The smoldering boundary of thin duff is more prone to losing ther-
145 mal energy to convective heat loss (Miyaniishi and Johnson 2002), thermal
146 energy that would otherwise be used to drive off moisture and sustain the
147 combustion process. The HCA model accounts for this phenomenon by in-
148 hibiting the amount of thermal energy imparted to the soil by scaling the
149 combustion temperature of the duff, T_c , by an *efficiency* factor that depends
150 upon the depth associated with the ignited cell (described in detail later).

151 **Temperature and Moisture Dynamics**

152 The HCA model employs a continuous model of heat and moisture dynamics
153 and the resulting system of partial differential equations is discretized. The
154 soil (duff) is treated as a mixture of various components, namely mineral
155 solids, organic solids, air, and water. The HCA model uses a modified
156 version of the heat and moisture transport model in mineral soil developed
157 by Campbell et al. (1994, 1995).

158 The HCA model modifies the model of Campbell et al. (1995) for a two-
159 dimensional fuel bed of duff instead of a one-dimensional soil column. Tem-
160 perature and moisture gradients drive both vertical and horizontal trans-

161 port of heat and moisture in porous media (de Vries 1958). Thus the one-
 162 dimensional vertical gradient $\frac{\partial}{\partial z}$ is replaced by the two-dimensional gradient
 163 operator $\nabla = \left(\frac{\partial}{\partial x}, \frac{\partial}{\partial y}\right)$. Taking convective cooling at the surface of the duff
 164 and mineral soil into account, the continuous model for heat and moisture
 165 transport is

$$(2) \quad C \frac{\partial T}{\partial t} - H d_w \frac{\partial \theta}{\partial t} = \nabla \cdot (K \nabla T) - \kappa_c C (T - T_a)$$

$$(3) \quad d_w \frac{\partial \theta}{\partial t} = -\nabla \cdot \left(\frac{V}{1 - \frac{p(T)}{P_a}} \nabla(p(T)) \right)$$

166 for (x, y) in the unconsumed region of duff. The convective cooling constant,
 167 κ_c (hr^{-1}), is taken to be 0.1, and T_a is the ambient temperature (293.15 K).
 168 Notice that in the absence of space and moisture considerations, Equation
 169 (2) reduces to Newton's Law of Cooling with κ_c as the cooling constant. The
 170 burned region is updated stochastically. A continuous rule is not developed
 171 for how this region changes through time. The rule governing how the
 172 burned region changes through time is more naturally accomplished in a
 173 discrete setting. The temperature T is measured with the Kelvin (K) scale,
 174 θ is the volumetric moisture content of the soil ($\text{m}^3 \text{ m}^{-3}$), C is the volumetric
 175 heat capacity of the soil ($\text{J m}^{-3} \text{K}^{-1}$), H is the latent heat of vaporization of
 176 water (J kg^{-1}), d_w is the density of liquid water (kg m^{-3}), p is the partial
 177 pressure of water vapor in the soil (Pa), P_a is ambient pressure (taken to be

178 standard pressure, 101,325 Pa), and V is the vapor conductivity of the soil
 179 ($\text{kg m}^{-1} \text{Pa}^{-1} \text{hr}^{-1}$). Note that the HCA model uses different time units
 180 than Campbell et al. (1995) since smoldering combustion is a very slow
 181 process (linear smolder velocities are on the order of $10^{-2} \text{ m hr}^{-1}$). The
 182 term $-Hd_w \frac{\partial \theta}{\partial t}$ accounts for transport of thermal energy due to water vapor
 183 moving through the soil. The term $1/(1 - \frac{p(T)}{P_a})$ is called the *Stefan correction*
 184 which is a mass flow correction that accounts for the flow of water vapor
 185 induced by the movement of air in the soil (Ghildyal and Tripathi 1987).
 186 Also, note that θ is the sum of the volumetric fractions of liquid water and
 187 precipitable water vapor (the volumetric fraction of condensed water vapor).

188 The thermal conductivity K (in $\text{J m}^{-1} \text{hr}^{-1} \text{K}^{-1}$) is determined by soil
 189 type. Since both the chemical and physical structure of peat are similar to
 190 forest duff, the HCA model assumes that the physical characteristics of peat
 191 including mass and thermal transport properties are similar enough to act as
 192 a surrogate for forest duff. A temperature-dependent thermal conductivity
 193 model for soil (Campbell et al. 1994; Hiraiwa and Kasubuchi 2000; Tarnawski
 194 et al. 2000; Balland and Arp 2005) is necessary since Frandsen (1991) notes
 195 that smoldering ground fires elevate underlying mineral soil to temperatures
 196 above 300°C with temperatures as high as 600°C . The HCA model uses the
 197 temperature-dependent model of Campbell et al. (1994) to estimate the
 198 thermal conductivity of duff. The parameters for peat are used with the
 199 thermal conductivity model of Campbell et al. (1994).

200 The vapor conductivity V of the soil is expressed by Campbell et al.
 201 (1995) as $V = \frac{\xi \eta (\pi - \theta) M_w D_v}{RT}$ where M_w is the molecular weight of water
 202 (kg mol^{-1}) and R is the universal gas constant (mol K^{-1}). The tortuosity

203 correction is given by ξ and is taken to be 0.66 (Campbell et al. 1995). The
 204 tortuosity of a soil is the ratio of the straight line distance from one location
 205 to another to how far a particle actually travels (Hillel 1998). The vapor
 206 flow enhancement factor η is a tuning parameter that is taken to be 1 for
 207 most mineral soil applications (Campbell et al. 1995; Hillel 1998). However,
 208 since this effort concerns moisture transport in duff, a different value is used
 209 (see implementation). The expression $\pi - \theta$ is the air filled pore space of
 210 the soil. The diffusivity of water vapor in air D_v ($\text{m}^2 \text{hr}^{-1}$) is given by
 211 $D_v = D_{v0}(\frac{P_0}{P_a})(\frac{T}{T_0})^{7/4}$ where D_{v0} is the diffusivity and P_0 is the ambient
 212 pressure at standard temperature and pressure.

213 An empirically derived equation used by Campbell et al. (1994) ex-
 214 presses the latent heat of vaporization in terms of temperature in the units
 215 of J mol^{-1} as $H = 45144 - 48(T - 273.15)$. The above is rescaled to J kg^{-1}
 216 by using the molecular weight of water.

217 Campbell et al. (1995) note that the relationship between p and θ is
 218 not unique. To account for this, the partial pressure of water is expressed
 219 as the product of relative humidity h and the saturation vapor pressure P
 220 (Pascals), $p = hP$. Campbell et al. (1995) note that the saturation vapor
 221 pressure of water is function of temperature alone and give an empirically
 222 derived formula for P in terms of T and is given by

$$P(T) = P_0 e^{13.3016S(T) - 2.042S(T)^2 + 0.26S(T)^3 + 2.69S(T)^4}$$

223 where $S(T) = 1 - \frac{373.15}{T}$. The humidity is expressed in terms of the tempera-
 224 ture of the soil as $h = e^{\frac{M_w \psi}{RT}}$, where ψ is the water potential (J kg^{-1}) of the

225 soil. The water potential for duff is allowed to vary between $\psi_{sat} = -10^{-2}$
 226 J kg^{-1} (for saturated duff where saturation is defined to occur when the
 227 volumetric fraction of water equals the porosity of dry duff) and $\psi_0 = -10^6$
 228 J kg^{-1} (for oven dry soil (Campbell et al. 1995)) according to the empirical
 229 relation $\psi(\theta) = a\theta^b$ for unsaturated soil where a and b are fitting param-
 230 eters (Hillel 1998). The points (θ_{min}, ψ_0) and $(\theta_{sat}, \psi_{sat})$ on the estimated
 231 water retention curve determine the estimates for a and b (the field con-
 232 ditions of spruce/pine duff given by Frandsen (1997) induce the parameter
 233 estimates $a = -0.0062$, $b = -4.1024$). By using this relation, the HCA
 234 model assumes that moisture transfer takes place in unsaturated duff, and
 235 that water potential depends solely upon moisture content. This is reason-
 236 able since duff consumption takes place primarily in an unsaturated range
 237 of moisture (Hille and Stephens 2005).

238 Since moisture content is used to update ignition probability, it becomes
 239 unnecessary to update after a cell is undergoing consumption. In smoldering
 240 and consumed regions θ is set to a specified minimum value θ_{min} (taken to
 241 be 0.01). In the smoldering regions the temperature is set to the scaled
 242 temperature at which duff undergoes combustion,

$$(T_c - T_a) \left(\frac{1}{1 + \varepsilon_1 e^{-\varepsilon_2 \tau_t^{i,j}}} \right) + T_a,$$

243 where the unscaled combustion temperature T_c (for deep duff) is taken to
 244 be 400°C (Miyanishi 2001). The efficiency factor, $\frac{1}{1 + \varepsilon_1 e^{-\varepsilon_2 \tau}}$, approaches
 245 1 as depth increases, indicating a maximum efficiency of the smoldering
 246 front to impart thermal energy to the soil where ε_1 and ε_2 are efficiency

247 parameters (respectively taken to be 9 and 150 since a maximum efficiency
248 of 1 is approached a depth of about 0.05 m). When extinction occurs,
249 the temperature decays to the ambient temperature according to Newton's
250 Law of Cooling. Temperature and VMC at the boundary of the domain
251 are assumed to be the ambient temperature and initial VMC. The above
252 establishes boundary conditions for the temperature and moisture dynamics
253 at the ever-changing boundary of unconsumed duff.

254 Equations (2) and (3) and the boundary conditions described above serve
255 as the continuous thermal and moisture transport model in unconsumed
256 duff. The model equations are discretized to develop update rules for duff
257 temperature and moisture on the cellular lattice described above resulting
258 in the HCA model. The discretization is accomplished by using a forward
259 difference in time and a centered difference in space.

260 **Implementation**

261 The HCA model was implemented in MATLAB using Monte Carlo methods
262 to simulate ignition probabilities determined by duff conditions. To improve
263 the run time and stability in the numerical scheme for solving equations (2)
264 and (3), several restrictions were imposed. The non-Laplacian terms were
265 ignored when expanding the right hand side of [2] into its component deriva-
266 tives. This change had little, if any, perceptible effect upon the behavior of
267 the model. The thermal conductivity was restricted to values between 900
268 (thermal conductivity of organic material) and $18,000 \text{ J m}^{-1} \text{ hr}^{-1} \text{ K}^{-1}$ (up-
269 per bound used by Campbell et al. (1995)). The volumetric moisture content
270 was also restricted to values no lower than θ_{min} . Since the model of Campbell

271 et al. (1995) predicts a buildup of moisture ahead of a heat pulse, followed by
272 decay, an additional restriction was made to eliminate this buildup; the up-
273 dated volumetric moisture content was not allowed to exceed the volumetric
274 moisture content of the previous time step so that moisture is a decreasing
275 function of time. Another restriction made was to let the ambient temper-
276 ature act as a lower bound when updating temperature. With a vapor flow
277 enhancement factor of 1, the unrestricted temperature calculations predicted
278 freezing temperatures in some cells (the numerical scheme still appeared to
279 be stable). However, by using a *reduced* vapor flow enhancement factor of
280 1/3, this phenomenon was greatly reduced, with the most extreme cooling
281 being only fractions of a degree below ambient temperature. Since duff is
282 composed mostly of organic solids which serve to increase water retention
283 (Koorevaar et al. 1983), this reduction is not unreasonable. Therefore, the
284 model assumes a reduced vapor flow enhancement factor of 1/3 in addition
285 to a setting a lower bound on temperature. Imposing this restriction affords
286 the user more flexibility in choosing a vapor flow enhancement factor since
287 the model behaves well even when resetting the vapor flow enhancement
288 factor back to 1.

289 To compare the HCA model to empirical and laboratory studies, uni-
290 form initial conditions were used since burn studies often use peat samples
291 of uniform composition (Frandsen 1987, 1991, 1998; Miyanishi 2001). For
292 all simulations, duff conditions were initialized to the field conditions for
293 bulk density and inorganic content for spruce/pine (*Picea/Pinus*) duff re-
294 ported by Frandsen (1997). Unless otherwise noted, each model run used

295 the regression coefficients for spruce/pine duff reported by Frandsen (1997).

296 **Results**

297 The coupled combustion state and heat and moisture dynamics (Figure 4)
298 predict that regions exposed to the smoldering front are significantly drier
299 than unexposed regions, that is, a drying region ahead of the smoldering
300 front.

301 The end stage of the smoldering process (when the process is allowed
302 to proceed until extinction) is seen in Figures 5 and 6. Four consecutive
303 simulations were run for moist duff conditions (105% GMC) using both
304 initial burn configurations. Each simulation was allowed to proceed until
305 extinction occurred.

306 The amount of duff consumed varies with the moisture and inorganic
307 ratio (the ratio of the mass of water and inorganic solids to organic mass).
308 The model was repeatedly run incrementing these parameters. For each run
309 the initial simulated duff conditions were set to be uniform as in Frandsen
310 (1987) and simulated bulk density for each run was the average field bulk
311 density (116 kg m^{-3}) for spruce/pine duff reported by Frandsen (1997).
312 The model was run for moisture ratios from 0 to 2 and inorganic ratios from
313 0 to 6, each in increments of 0.1 and the average proportion of duff consumed
314 over fifty trials was recorded.

315 The simulated smolder velocity was measured using the same method
316 described in the model formulation, with the exception that the dynamic
317 duff conditions also determined the spread probability. Fifty trials were

318 conducted and then averaged to produce a predicted simulated smolder ve-
319 locity at each combination of inorganic and moisture ratio (Figure 8).

320 To test whether or not depth has any effect on duff consumption, the
321 model was run for varying depth and volumetric moisture content and the
322 average proportion of duff consumed over fifty trials was recorded for each
323 combination of these. The results clearly demonstrate that depth does af-
324 fect the behavior of the model, with increasing depth resulting in sustained
325 smoldering propagation at higher moisture contents (Figure 9).

326 Discussion

327 In order to accurately model the spatial patterns observed in a smoldering
328 ground fire, the phenomenon of a drying front in duff is a key aspect this
329 model seeks to capture. The simulated temperature distribution (Figure
330 4) displays isolated patches of smoldering combustion indicating qualitative
331 agreement with thermal images of actual smoldering ground fires. In the
332 field, unburned “islands” of duff are commonly observed (Miyanishi and
333 Johnson 2002; Knapp and Keeley 2006); the HCA model predicts this phe-
334 nomenon near the limits of smoldering combustion (Figure 6).

335 The results of the simulations predicting limits of smoldering combustion
336 (Figure 7) are qualitatively similar to empirical results found in Frandsen
337 (1987) in which peat samples with known uniform composition were exposed
338 to an ignition source and a result of burn/no burn was recorded. Frandsen
339 observed that the limits of smoldering combustion are described well by a line
340 of negative slope with positive intercepts. The HCA model predicts a similar

341 response in spruce/pine duff where the limits of smoldering combustion are
342 similarly described (Figure 7).

343 It is apparent that there is overall qualitative agreement between the
344 simulated smolder velocities and the smolder velocity predicted by the sta-
345 tistical model of Frandsen (1991). However, the delayed effect of the in-
346 organic ratio accounted for in Frandsen's model is not present in the HCA
347 model; Frandsen's predicted smolder velocity is not affected by the inorganic
348 ratio until it reaches a value of 1. Also, the simulated smolder velocity does
349 not appear to decrease until close to the limits of smoldering combustion
350 where it then falls off rather sharply, whereas Frandsen's model predicts a
351 linearly decreasing smolder velocity up to and past the limits of smoldering
352 combustion. Also, Frandsen's model predicts a maximum smolder velocity
353 of about 0.025 m hr^{-1} , whereas, the HCA model simulates a slightly larger
354 maximum smolder velocity of about 0.028 m hr^{-1} .

355 Although the model is two-dimensional, it accounts for the effect of depth
356 (third-dimension) as well by means of the efficiency function describing ef-
357 ficiency versus depth, described in the methods section. The smoldering
358 perimeter more effectively transmits heat to the unconsumed duff due to
359 less heat being carried off by convection (Miyaniishi and Johnson 2002). The
360 results suggest that increasing duff depth allows for sustained combustion at
361 higher moisture contents which is in line with empirical studies (Miyaniishi
362 and Johnson 2002).

363 With increasing depth, the efficiency with which the smoldering front im-
364 parts thermal energy to the unconsumed duff also increases (with a limiting
365 value of 1) (Figure 9). Since the relationship between depth and efficiency

366 is assumed to be a strictly increasing relationship, depth indirectly accounts
367 for efficiency. Hence, at an efficiency (depth) near zero, the temperature has
368 very little effect with little moisture being driven off ahead of the front. As
369 the maximum efficiency is approached (deeper duff), however, the tempera-
370 ture takes effect and drives off more moisture ahead of the front so that more
371 duff is consumed. Thus, temperature and moisture dynamics are worthy of
372 consideration in any spatially explicit model of duff consumption.

373 Modeling the fuel bed as a lattice of cells offers multiple advantages.
374 Stochastic and deterministic models are easily coupled and integrated into
375 the model. Also, improved models (along with their numerical implementa-
376 tion) for the various phenomena considered (particularly heat and moisture
377 transport) are easily integrated into the model. Additionally, modifications
378 are easily made to the model to answer other important questions concerning
379 duff consumption.

380 By considering stand characteristics such as tree stem density, stem and
381 crown diameters, and how duff depth and moisture vary in relation to these
382 quantities (Hille and Stephens 2005), an L by L meter area of forest may be
383 simulated by stochastically initializing both of the above quantities jointly
384 with duff characteristics. Once a rule is established for how contact with
385 smoldering duff influences whether or not a tree dies (by duration of and
386 area of exposure, bark thickness, temperature of smoldering, etc.), a ground
387 fire may be simulated and an estimate of tree mortality caused by exposure
388 to smoldering duff may be generated by repeated simulation.

389 Organic bulk density, mineral content, moisture content and thickness
390 of the duff layer may be stochastically initialized for each cell to simulate a

391 typical fuel bed found in the field. The model encounters instabilities with
392 large variation in organic bulk density, a shortcoming that may be remedied
393 by neglecting the volumetric fraction of air in the duff when calculating
394 volumetric heat capacity.

395 The two-dimensional lattice of cells can also model a vertical cross sec-
396 tion of duff rather than a horizontal layer as presented here. With minor
397 modifications taking orientation and the heterogeneity of the various organic
398 soil horizons into account, repeated simulation could predict duff depth re-
399 duction under a known set of conditions. Unlike the model representing a
400 horizontal duff layer, the influence of the distinct structural differences be-
401 tween the duff horizons upon heat and mass transport could be explicitly
402 accounted for, particularly differences in quantities such as bulk density (af-
403 fecting the air-filled pore space (Ochsner et al. 2001)) that influence mass
404 and thermal transport. Repeated simulation of the model would not only
405 offer mean and variance estimates of duff depth reduction, but would also
406 predict a distribution for duff depth reduction. A one-dimensional lattice
407 model of a soil column might also be considered. Duff depth reduction could
408 also be estimated by introducing a slight modification to the model in which
409 the depth of each cell decreases in a probabilistic fashion (Holt 2008).

410 The HCA model could also be useful in predicting the effects of pre-
411 scribed burning on post-burn spatial heterogeneity. Fuel continuity caused
412 by fire exclusion and the consequent lack of spatial heterogeneity in fuels
413 and vegetation is favorable to some organisms, particularly those that flour-
414 ish in duff. However, tree and herbaceous species that do not establish well
415 on duff are in some cases virtually unable to propagate (Miyaniishi 2001)

416 which illustrates how a lack of spatial heterogeneity can lead to decline in
417 biological diversity (Knapp and Keeley 2006). Thus spatial heterogeneity,
418 as measured by the variability and “patchiness” in ground cover, canopy
419 cover, and other structural characteristics, is an important index of forest
420 health. Low fuel loads believed to exist before fire exclusion are believed to
421 have resulted in greater spatial heterogeneity in vegetation and fuels (Knapp
422 and Keeley 2006). Knapp and Keeley (2006) showed that it is possible to
423 approximate the degree of spatial heterogeneity believed to exist before fire
424 exclusion suggesting that computer models would be useful in predicting
425 the degree of post-burn heterogeneity. Patch size distributions generated by
426 the model developed here offer measures of spatial heterogeneity in ground
427 fuels. The HCA model in conjunction with pair approximation techniques
428 reviewed by Sato and Iwasa (2000) used to analyze spatial heterogeneity in
429 lattice models may also prove to be a powerful combination in predicting
430 and characterizing spatial heterogeneity in ground fuels.

431 **Conclusions**

432 The HCA model of smoldering propagation in forest floor duff is easy to use,
433 non-site-specific, and spatially and temporally accurate. The model predicts
434 expected qualitative features concerning spatial patterns of duff consump-
435 tion. The qualitative agreement with laboratory and field studies affirms
436 that spatial patterns predicted by the model are indeed valid. A particu-
437 larly appealing aspect of the model is that it is versatile. It is a general
438 model from which a site-specific model may be developed by considering a

439 small number of easily measured, but key, parameters. The versatility of the
440 model is not limited to its generality; the model is easily modified to account
441 for other phenomena important to management and ecology, particularly,
442 tree mortality, duff depth reduction, and post-burn spatial heterogeneity.
443 These potential models, when incorporated into models concerning other
444 aspects of prescribed and wildfire, could help foresters and ecologists better
445 understand and simulate a process that has profound implications for forest
446 health.

Acknowledgements

We gratefully acknowledge G.S. Campbell for correspondence that helped greatly in implementing the heat and moisture dynamics used by the HCA model. We also acknowledge Megan Higgs for assistance with the reporting of statistical issues in this article. J. Morgan Varner was supported by funds from the USDA McIntire-Stennis Research Program.

References

- Balland, V. and Arp, P.A. 2005. Modeling soil thermal conductivities over a wide range of conditions. *J. Environ. Eng. Sci.* 4: 549–558.
- Bradbury, A.G., Sakai, Y., and Shafizadeh, F. 1979. A kinetic model for the pyrolysis of cellulose. *J. Appl. Polymer Sci.* 23: 3271–3280.
- Campbell, G.S., Jungbauer, J.D., Bidlake, W.R., and Hungerford, R.D.

1994. Predicting the effect of temperature on soil thermal conductivity. *Soil Science* 158: 307–313.
- Campbell, G.S., Jungbauer, J.D., Bristow, K.L., and Hungerford, R.D. 1995. Soil temperature and water content beneath a surface fire. *Soil Science* 159: 363–374.
- de Vries, D.A. 1958. Simultaneous transfer of heat and moisture in porous media. *Trans. Am. Geophys Union* 39: 909–916.
- Durrett, R. 1999. Stochastic spatial models. *SIAM Review* 41: 677–718.
- Fonda, R. and Varner, J.M. 2004. Burning characteristics of cones from eight pine species. *Northwest Science* 78(4): 322–333.
- Frandsen, W.H. 1987. The influence of moisture and mineral soil on the combustion limits of smoldering forest duff. *Can. J. For. Res.* 17: 1540–1544.
- Frandsen, W.H. 1991. Burning rate of smoldering peat. *Northwest Science* 65: 166–172.
- Frandsen, W.H. 1997. Ignition probability of organic soils. *Can. J. For. Res.* 27: 1471–1477.
- Frandsen, W.H. 1998. Heat flow measurements from smoldering porous fuel. *Int. J. Wildland Fire* 8: 137–145.
- Gerlee, P. and Anderson, A. 2007. An evolutionary hybrid cellular automaton model of solid tumour growth. *Journal of Theoretical Biology* 247: 583–603.

- Ghildyal, B.P. and Tripathi, R.P. 1987. Soil Physics. Wiley Eastern Limited, New Delhi, India.
- Hiers, J.K., O'Brien, J.J., Will, R.E., and Mitchell, R.J. 2007. Forest floor depth mediates understory vigor in xeric *Pinus palustris* ecosystems. *Ecological Applications* 17: 806–814.
- Hille, M.G. and Stephens, S.L. 2005. Mixed conifer forest duff consumption during prescribed fires: Tree crown impacts. *Forest Science* 51: 417–424.
- Hillel, D. 1998. Environmental Soil Physics. Academic Press.
- Hiraiwa, Y. and Kasubuchi, T. 2000. Temperature dependence of thermal conductivity of soil over a wide range of temperature. *Eur. J. Soil Sci.* 51: 211–218.
- Holt, B.V. 2008. A Stochastic Spatial Model for the Consumption of Organic Forest Soils in a Smoldering Ground Fire. Master's thesis, Humboldt State University.
- Knapp, E.E. and Keeley, J.E. 2006. Heterogeneity in fire severity within early season and late season prescribed burns in a mixed-conifer forest. *Int. J. Wildland Fire* 15: 37–45.
- Koorevaar, P., Menelik, G., and Dirksen, C. 1983. Elements of Soil Physics. *Developments in Soil Science*, 13. Elsevier.
- Miyanishi, K. 2001. Duff consumption. In *Forest Fires-Behavior and Ecological Effects*, pages 437–474. Academic Press, San Diego, CA.

- Miyanishi, K. and Johnson, E.A. 2002. Process and patterns of duff consumption in the mixedwood boreal forest. *Can. J. For. Res.* 32: 1285–1295.
- Ochsner, T.E., Horton, R., and Ren, T. 2001. A new perspective on soil thermal properties. *Soil Sci. Soc. Am. J.* 65: 1641–1647.
- Ohlemiller, T.J. 2002. NFPA HFPE-02;SFPE Handbook of Fire Protection Engineering, chapter 9, Smoldering Combustion, pages 2/200–2/210. 3rd edition. BFRP Publications.
- Ross, S. 2005. *A First Course in Probability*. 7th edition. Prentice Hall.
- Ryan, K.C. and Frandsen, W.H. 1991. Basal injury from smoldering fires in mature *Pinus ponderosa* Laws. *Int. J. Wildland Fire* 1: 107–118.
- Sato, K. and Iwasa, Y. 2000. Pair approximations for lattice-based ecological models. In *The Geometry of Ecological Interactions: Simplifying Spatial Complexity*, pages 341–358. Cambridge University Press.
- Swezy, D.M. and Agee, J.K. 1991. Prescribed-fire effects on fine-root and tree mortality in old-growth ponderosa pine. *Can. J. For. Res.* 21: 626–634.
- Tarnawski, V.R., Gori, F., Wagner, B., and Buchan, G.D. 2000. Modeling approaches to predicting thermal conductivity of soils at high temperatures. *Int. J. Energy Res.* 24: 403–423.
- Varner, J.M., Gordon, D.R., Putz, F.E., and Hiers, J.K. 2005. Restoring fire to long-unburned *Pinus palustris* ecosystems: Novel fire effects and

consequences for long-unburned ecosystems. *Restoration Ecology* 13: 536–544.

Varner, J.M., Hiers, J.K., Ottmar, R.D., Gordon, D.R., Putz, F.E., and Wade, D.D. 2007. Overstory tree mortality resulting from re-introducing fire to long-unburned long leaf pine forests: the importance of duff moisture. *Can. J. For. Res.* 37: 1349–1358.

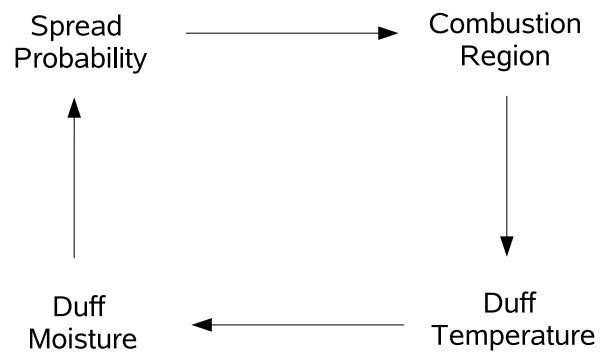


Figure 1: Overall model structure for predicting the spatial pattern of forest floor duff consumption.

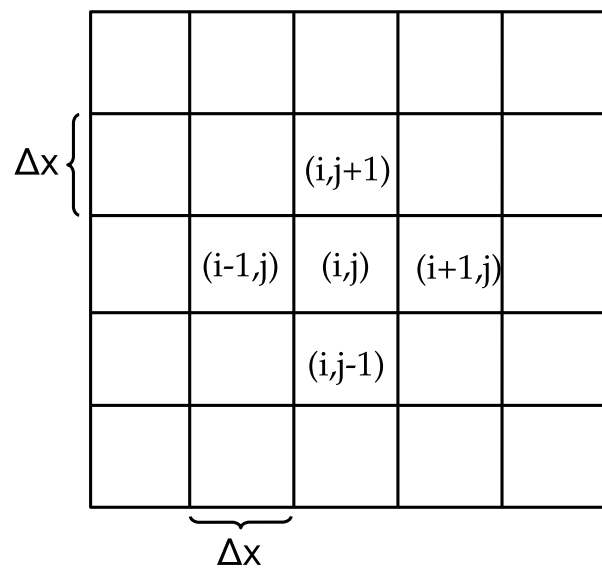


Figure 2: Cell (i, j) and its four nearest neighbors representing the cellular automaton approach used here to model smoldering propagation in forest floor duff.

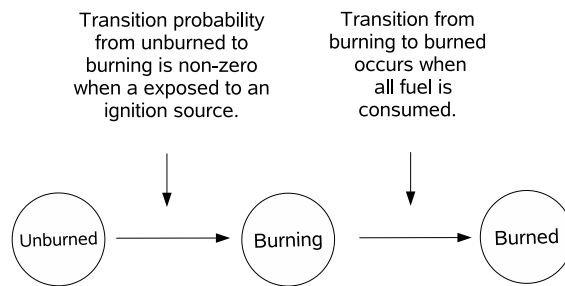


Figure 3: Three stage model of the combustion process in forest floor duff.

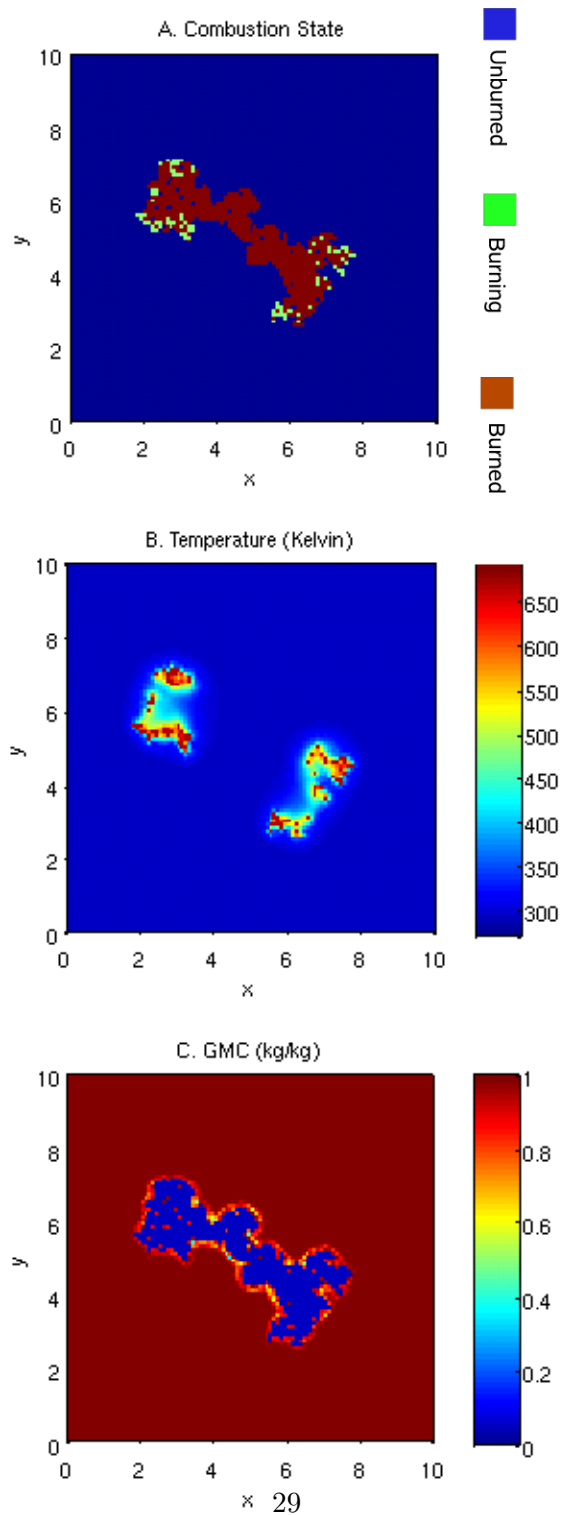


Figure 4: Simulated combustion, heat, and moisture dynamics of forest floor duff using a hybrid cellular automaton model. The predicted drying front is seen in panel C displaying moisture content across space. $\gamma = 1 \text{ kg kg}^{-1}$, $\rho = 116 \text{ kg m}^{-3}$, $\alpha = 0.307 \text{ kg kg}^{-1}$, and $\tau = 0.15 \text{ m}$.

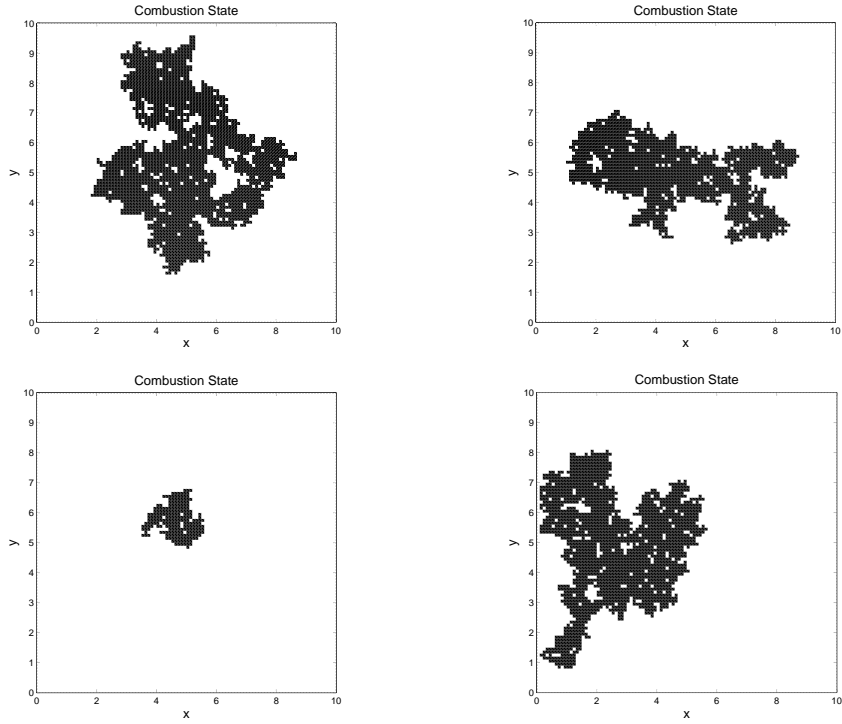


Figure 5: The resulting burn pattern for four consecutive model runs with very moist duff allowing the simulation to proceed until extinction. Ignition was initiated in the center for each run. The initial duff conditions were $\gamma = 1.05 \text{ kg kg}^{-1}$, $\rho = 116 \text{ kg m}^{-3}$, $\alpha = 0.307 \text{ kg kg}^{-1}$, and $\tau = 0.15 \text{ m}$.

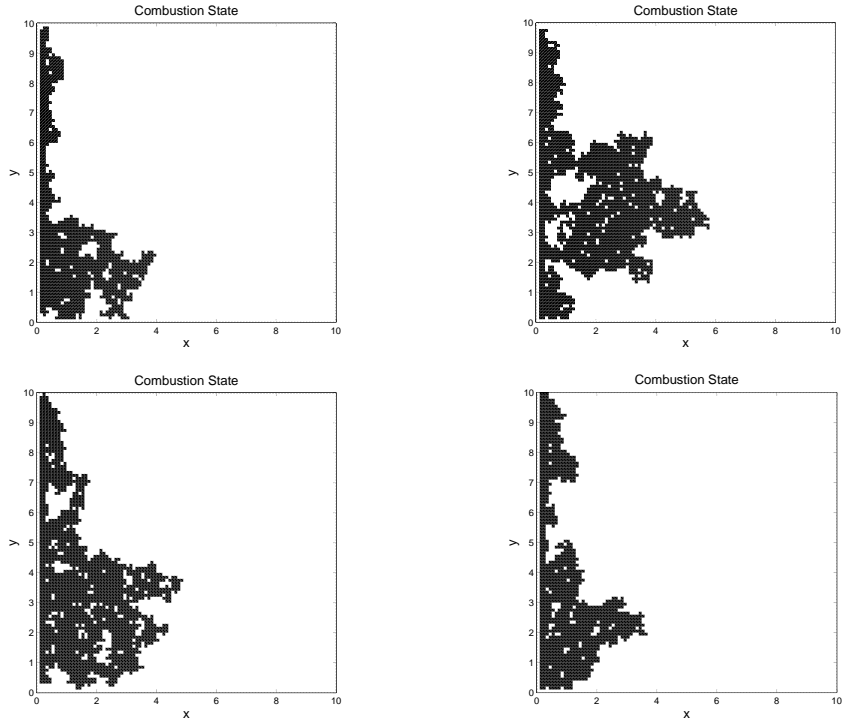


Figure 6: The resulting burn pattern for four consecutive model runs with very moist duff allowing the simulation to proceed until extinction. Ignition was initiated at the left edge for each run. The initial duff conditions were $\gamma = 1.05 \text{ kg kg}^{-1}$, $\rho = 116 \text{ kg m}^{-3}$, $\alpha = 0.307 \text{ kg kg}^{-1}$, and $\tau = 0.15 \text{ m}$.

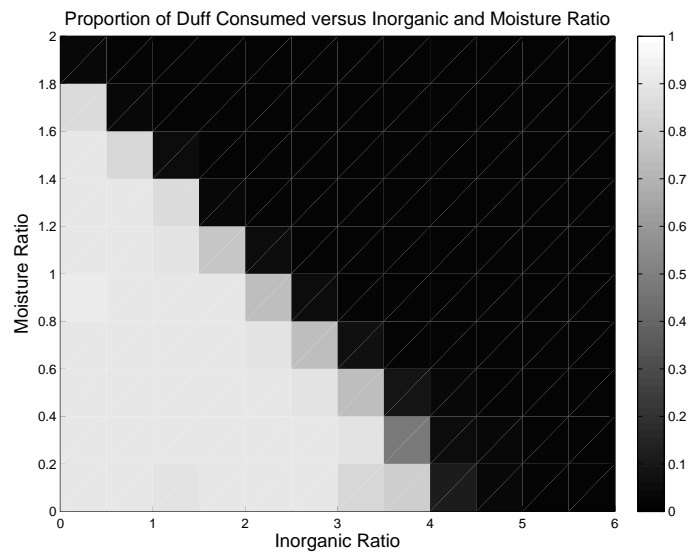


Figure 7: The proportion of a simulated 10m by 10m patch of spruce/pine duff consumed by smoldering combustion expressed in terms of inorganic and moisture ratio. Each point represents the average of fifty trials. $\rho = 116 \text{ kg m}^{-3}$, $\tau = 0.15 \text{ m}$.

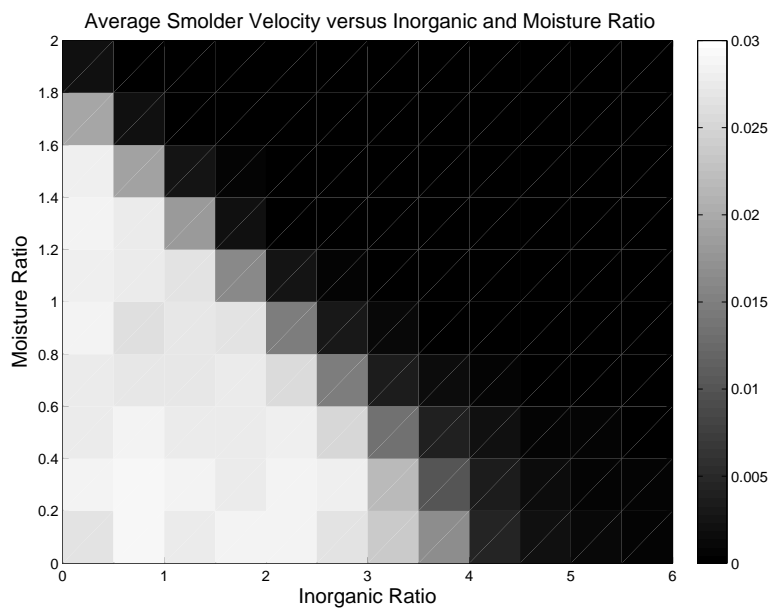


Figure 8: Simulated smolder velocities for spruce/pine duff, $\rho = 116 \text{ kg m}^{-3}$, $\tau = 0.15 \text{ m}$. Each point represents the average of fifty trials.

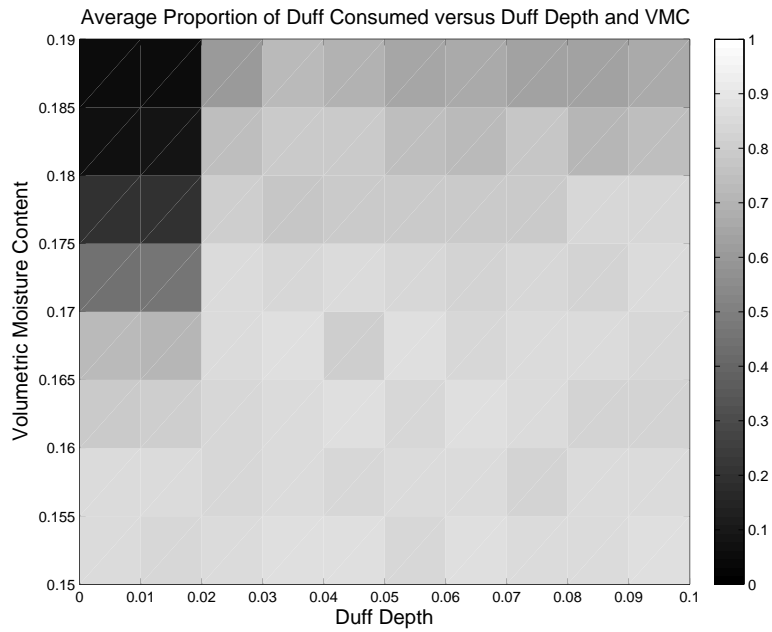


Figure 9: The average proportion of a simulated 1m by 1m patch of spruce/pine duff consumed completely by smoldering combustion expressed in terms of initial duff depth and volumetric moisture content. Ignition was initiated at the left edge. Each point represents the average of fifty trials. $\rho = 116 \text{ kg/m}^3$, $\alpha = 0.307 \text{ kg/kg}$.